เอกสารอ้างอิง

1. T. Bovonratanaraks, D. R. Allan, S. A. Belmonte, M. I. Mcmahon and R. J. Nelmes, *Phys. Rev. B* **73**, 144112 (2006).
2. H. Olijnyk and W. B. Holzapfel, *Phys. Lett. A* **100**, 191 (1984).
3. H. L. Skriver, *Phys. Rev. Lett.* **49**, 1768 (1982).
4. R. Ahuja, B. Johansson, and O. Eriksson, *Phys. Rev. B* **58**, 8152 (1998).
5. F. Jona and P. M. Marcus, *J. Phys.: Condens. Matter* **18**, 4623 (2006).
6. R. H. Mutlu, *Phys. Rev. B* **54**, 16321 (1996).
7. V. L. Sliwko, P. Mohn, K. Schwarz and P. Blaha, *J. Phys.: Condens. Matter* **8**, 799 (1996).
8. M. Winzenick and W. B. Holzapfel, *Phys. Rev. B* **53**, 2151 (1996).
9. D. R. Allan, R. J. Nelmes, M. I. McMahon, S. A. Belmonte and T. Bovonratanaraks, *Rev. High Pressure Sci. Technol.* **7**, 236 (1998).
10. M. I. McMahon, T. Bovornratanaraks, D. R. Allan, S. A. Belmonte, and R. J. Nelmes, *Phys. Rev. B* **61**, 3135 (2000).
11. A. Phusittrakool, T. Bovornratanaraks, R. Ahuja and U. Pinsook, *Phys. Rev. B* **77**, 174118 (2008).
12. V.G. Vaks and A.Y. Trefilov, *Phys. Lett. A* **127**, 37 (1988).
13. V.G. Vaks, M.I. Katsnelson and A.V. Trefilov, *J. Phys.: Condens. Matter* **3**, 1409 (1991).
14. Y. Xie, J.S.Tse and G. Zou, *Phys. Rev. B* **75**, 064102 (2007).
15. Y. Xie, Y.M. Ma and G.T. Zou, *New J. Phys.* **10**, 063022 (2008).
16. S. Mizobata, T. Matsuoka and K. Shimizu, *J. Phys. Soc. Jpn.* **76**, Suppl. A 23 (2007).
17. G. Kresse and J. Hafner, *Phys. Rev. B* **47**, 558 (1993); G. Kresse and J. Furthmüller, *Phys. Rev. B* **54**, 11169 (1996).
18. P.E. Blöchl, *Phys. Rev. B* **50**, 17953 (1994); G. Kresse, and J. Joubert, *Phys. Rev. B* **59**, 1758 (1999).
19. J.P. Perdew and Y. Wang, *Phys. Rev. Lett.* **45**, 13244 (1992).
20. F. Birch, *Phys. Rev.* **71**, 809 (1947).
21. J. Donohue, *The Structure of the Elements*, New York: Wiley (1974).
22. W. B. Pearson, *A Handbook of Lattice Spacing and Structures of Metals and Alloys vol* 2, Oxford: Pergramon (1967).
23. E. A. Brandes and G. B. Brook, *Smithells Metals Reference Book*, 7th ed, Oxford: Butterworth-Heinemann (1992).

สำนักงานคณะกรรมการวิจัยแห่งชาติ ห้องสมุดงานวิจัย

24. L. Pollack, J. P. Perdew, J. He, M. Marques, F. Nogueira and C. Fiolhais, *Phys. Rev. B* **54**, 4519 (1996).

25. D. B. McWhan and A. Jayaraman, *Appl. Phys. Lett.* **3**, 129 (1963).

26. J. Mizuki and C. Stassis, *Phys. Rev B* **35**, 8372 (1985).

27. H. Katzke and P. Toledano, *Phys. Rev. B* **75**, 174103 (2007).

บทความวิจัยที่เป็นผลงานจากแผนงานวิจัยวัสดุภายใต้สภาวะรุนแรง

IOP PUBLISHING JOURNAL OF PHYSICS: CONDENSED MATTER

J. Phys.: Condens. Matter **22** (2010) 355801 (4pp) doi:10.1088/0953-8984/22/35/355801

High pressure orthorhombic structure of $CuInSe_2$

T Bovornratanaraks[1,2], V Saengsuwan[1], K Yoodee[1,2], M I McMahon[3], C Hejny[3] and D Ruffolo[2,4]

[1] Department of Physics, Faculty of Science, Chulalongkorn University, Bangkok, 10330, Thailand

[2] ThEP Centre, CHE, 328 Si-Ayutthaya Road, Bangkok, 10400, Thailand

[3] School of Physics and Centre for Science at Extreme Conditions, The University of Edinburgh, Mayfield Road, Edinburgh EH9 3JZ, UK

[4] Department of Physics, Faculty of Science, Mahidol University, Bangkok, 10400, Thailand

E-mail: thiti.b@chula.ac.th

Received 2 May 2010, in final form 13 July 2010
Published 10 August 2010
Online at stacks.iop.org/JPhysCM/22/355801

Abstract

The structural behaviour of $CuInSe_2$ under high pressure has been studied up to 53 GPa using angle-dispersive x-ray powder diffraction techniques. The previously reported structural phase transition from its ambient pressure tetragonal structure to a high pressure phase with a NaCl-like cubic structure at 7.6 GPa has been confirmed. On further compression, another structural phase transition is observed at 39 GPa. A full structural study of this high pressure phase has been carried out and the high pressure structure has been identified as orthorhombic with space group $Cmcm$ and lattice parameters $a = 4.867(8)$ Å, $b = 5.023(8)$ Å and $c = 4.980(3)$ Å at 53.2(2) GPa. This phase transition behaviour is similar to those of analogous binary and trinary semiconductors, where the orthorhombic $Cmcm$ structure can also be viewed as a distortion of the cubic NaCl-type structure.

(Some figures in this article are in colour only in the electronic version)

1. Introduction

The ternary I–III–VI_2 compound semiconductor copper indium diselenide ($CuInSe_2$) is an analogue of the binary II–VI compound semiconductors. Despite much experimental and theoretical interest in this compound [1–4], very few high pressure studies have been carried out experimentally [5, 6]. This material has attracted much attention because of its variety of potential applications, especially as a candidate material for the fabrication of high-efficiency crystalline solar cells [7]. High pressure crystal structures have played an important role in governing electrical and optical properties of materials, which have a direct effect for photovoltaic applications [6]. In previous high pressure energy-dispersive powder diffraction studies of this material, a structural phase transition from the ambient tetragonal chalcopyrite phase to the face-centred cubic NaCl structure at 7.6 GPa have been reported [5]. This NaCl phase exists up to 29 GPa, the highest pressure obtained in that experiment. However, the peak intensities measured using energy-dispersive techniques were not suitable for Rietveld analysis. Therefore, full structure refinement could not be performed and the previously reported NaCl-type structure was deduced from the similarity between $CuInS_2$ and $CuInSe_2$ for the powder diffraction profiles and volume reduction at the transition pressure [5].

We have embarked on a re-examination of the high pressure structures and transitions in $CuInSe_2$ using angle-dispersive powder diffraction techniques with the image-plate detector on station 9.1 at the Synchrotron Radiation Source (SRS) at the Daresbury Laboratory, UK. We find the same structural phase transition at 7.1 GPa as has been previously reported [5]. On further compression, we have obtained extensive data through another phase transition at 39.2 GPa. This newly discovered phase has now been identified as an orthorhombic distortion of the NaCl structure and is stable up to 53.2 GPa, the maximum pressure reached in this experiment.

2. Experimental details

Single crystals of $CuInSe_2$ were grown by the horizontal directional freezing method. The growth process was slightly

 © 2010 IOP Publishing Ltd Printed in the UK & the USA

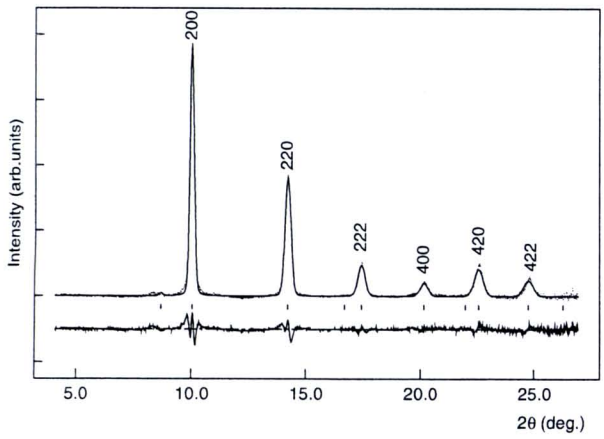

Figure 1. The full Rietveld refinement of the cubic structure at 8.7 GPa. The dotted line shows the observed profile and the solid line shows the calculated profile. The tick marks below the profiles show the calculated peak positions and the difference between the observed and calculated profiles is indicated under the tick marks.

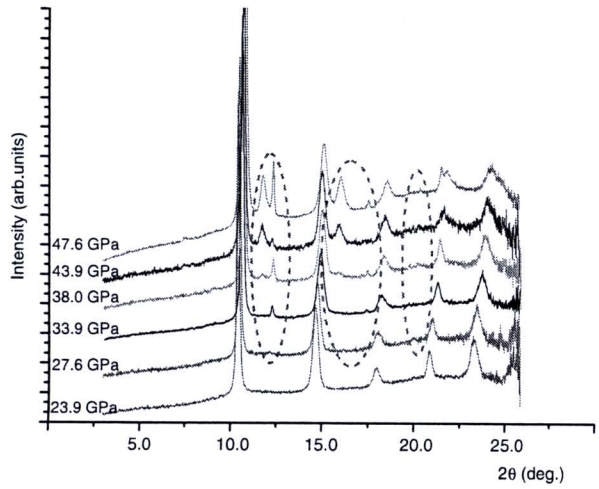

Figure 2. The diffraction patterns collected under pressures between 23.9 and 47.6 GPa. The newly appearing reflections from the orthorhombic phase are indicated by circles.

different from that normally employed elsewhere in that the melt was kept initially at 1523 K. The top free surface of the first half of the ingot showed the 112 plane along a length of a few centimetres. Crack free samples of centimetre size can be cut parallel to the free surface. In this particular batch, the p-type single crystal was found to be of very high quality, both with regard to the crystallinity and electrical properties [9]. X-ray powder diffraction showed sharp diffraction peaks of the clean chalcopyrite structure with $a = 5.7783$ Å and $c = 11.5716$ Å, giving $c/a = 2.0026$. The composition of the crystal, determined by EDS analysis, is 24.4% Cu, 23.7% In and 51.9% Se, which is slightly Cu-rich. The composition is slightly different from the reported [8] preferred composition of 23.5:26.4:50.1 for a large single crystal grown by the vertical Bridgeman method. The first attempt toward a high pressure structural solution was carried out using single-crystal techniques. However, the high quality single-crystal sample was pulverized upon compression. The sample was then finely ground for powder diffraction experiment. Diffraction data were collected on station 9.1 at the SRS using a wavelength of 0.4654 Å. The two-dimensional powder patterns collected on the image plate were read on a Molecular Dynamics 400A PhosphorImager and then integrated to give conventional one-dimensional diffraction profiles. Details of our experimental setup and pattern integration program have been reported previously [10]. The full conical aperture Diacell DXR-5 and DXR-6 were used, with diamond culet diameters of 200 and 300 μm respectively [11]. Samples were loaded with a 4:1 mixture of methanol:ethanol as the pressure-transmitting medium, and the pressure was measured using the ruby-fluorescence technique [12]. All structural parameters, including lattice parameters, were obtained from Rietveld refinement of the full integrated profiles using the program GSAS [13].

3. Results and discussion

Ambient temperature–pressure diffraction data were collected to ensure the purity of the powder sample after grinding. The verified samples were then pressurized and put back on the beamline for high pressure measurements. The diffraction pattern collected at ambient pressure showed a very smooth and contaminant free two-dimensional Debye–Scherrer pattern, which can be identified with the tetragonal chalcopyrite $I\bar{4}2d$ structure. On pressure increase the well-known transition from the tetragonal $I\bar{4}2d$ phase to the NaCl phase was observed at 7.1 GPa. However, the diffraction patterns observed for the cubic phase indicate a highly textured powder sample, with substantial intensity variation around the rings. In order to obtain a smooth one-dimensional diffraction profile, a textured sample in the cubic phase was annealed at 453 K for 10 h. The resulting smoother diffraction rings were then used for structure refinement. In order to confirm the structural detail of this high pressure phase, full Rietveld refinement has been performed on powder diffraction profiles collected over the entire pressure range of this phase. The diffraction patterns are contamination free and the full structural detail can be extracted. The first attempt to confirm the reported cubic structure has been carried out. Figure 1 shows the Rietveld refinement of the high pressure cubic structure collected at 8.7 GPa.

The diffraction profiles were collected throughout the first phase transition and beyond 29 GPa, the previous highest pressure reported, and found a new transition at 39 GPa. Figure 2 shows the evolution of the diffraction profile collected at various pressures through the phase transition at the high pressure region. The newly emerging reflections are indicated by circles. From the angle-dispersive patterns, full structural refinement can be performed and the cubic phase has now been confirmed by our experiment. On further compression, we observed a structural phase transition at 39.0 GPa and we have obtained data throughout the phase transition and

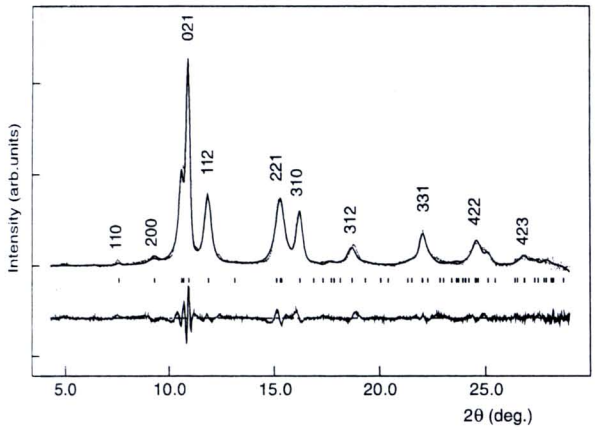

Figure 3. The Rietveld refinement of the diffraction pattern collected at 53.2 GPa. The dotted line shows the observed profile and the solid line shows the calculated profile. The tick marks below the profiles show the calculated peak positions and the difference between the observed and calculated profiles is indicated under the tick marks.

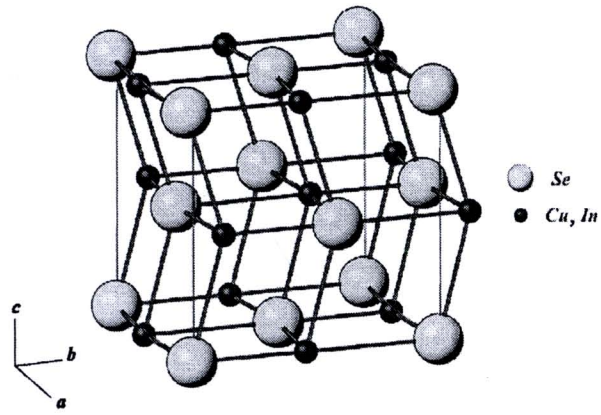

Figure 4. The crystal structure of the high pressure phase III of $CuInSe_2$, which can be considered an orthorhombically distorted NaCl structure.

the high pressure phase. The highest pressure reached in this experiment was 53.2 GPa. The structural solution of this newly discovered phase has been carried out. From the integrated diffraction profiles, the high pressure patterns reveal an obvious evolution from the cubic structure. This progression can also be clearly observed from the two-dimensional data recorded on the image plate. Therefore, for the third phase, a structural distortion from the cubic NaCl structure is expected. Based on this information, we have performed the *ab initio* indexing of this high pressure structure.

In the pattern collected at 53.2 GPa, it was possible to measure the positions of ten reflections, including the very weak reflection at 7.5°. Using the indexing program DICVOL [14], an excellent fit to the data was found to be given by an orthorhombic unit cell with lattice parameters of $a = 4.86$ Å, $b = 5.02$ Å and $c = 4.97$ Å. The pattern could then be indexed, and this revealed reflections with $h + k =$ odd in all (hkl) and $l =$ odd in $(h0l)$ to be systematically absent. The lattice symmetry is thus C-face centred. It is worth noting that only the very weak reflection (110) rules out two space groups, $C2cb$ and $Cmca$. The systematic absence conditions given above restrict possible space groups to $Cmcm$, $C2cm$ and $Cmc2_1$.

Full structural refinements have been carried out for all three possible space groups. The $Cmcm$, $C2cm$ and $Cmc2_1$ groups gave identical fit to all of our high pressure data collected at this phase. The highest-symmetry $Cmcm$ has been selected for further full structural analysis. The best fit to the $Cmcm$ structure, with R_{wp} factor = 0.0163, is shown in figure 3 with refined lattice parameters $a = 4.867(8)$ Å, $b = 5.023(8)$ Å and $c = 4.980(3)$ Å. The required systematic absence corresponds to the 4(c) position of $Cmcm$ $(0, y, 1/4;\ 0, -y, 3/4;\ 1/2, 1/2 + y, 1/4;\ 1/2, 1/2 - y, 3/4)$ with y(Cu–In) = 0.701(5) and y(Se) = 0.159(6). The structure can be considered as a distortion of the NaCl structure. From figure 4, it can be seen that the $Cmcm$ structure becomes the NaCl structure if lattice parameters are all equal, $y = 3/4$ and $1/4$. If $\Delta y \neq 0.5$, then there are displacement of alternate (001) planes in the [010] direction.

The refined lattice parameters of the high pressure cubic structure at 7.4 GPa is $a = 3.7205$ Å. The volume decrease (per formula unit), $\Delta V/V_0$, at the tetragonal–cubic transition is 11%. The unit cell of the orthorhombic $Cmcm$ structure immediately after the transition is $a = 4.897(5)$ Å, $b = 5.091(5)$ Å and $c = 5.025(4)$ Å, implying a further volume decrease of ~1%, and hence the total volume change for the two transitions is 12%.

Under high pressure, the ionicity becomes greater as the atomic separation decreases. The ionicity causes significant changes in the properties of semiconductors [18]. A larger ionicity affects the Coulomb interaction between ions and also the energy of the fundamental gap in the electronic band structure. When the ionicity is large enough, the material becomes a metal. The increasing Coulomb interaction between ions causes an increase in the cohesive energy of the crystal which favours the high-symmetry structure of the increasing coordinate [19]. In the case of $CuInSe_2$, its greater ionicity favours the $Cmcm$ structure containing eight-fold coordinated atoms and the rock-salt structure containing six-fold coordinated atoms rather than tetrahedral bonds in the chalcopyrite structure. The recovered phase is of zincblende-type, due to the residual disordered arrangement between the Cu and In atoms in the cubic phase. This was also observed by Tinoco *et al* [5].

4. Conclusions

In conclusion, our studies have concentrated on high pressure structures of the ternary-compound semiconductor, $CuInSe_2$. This is the first time that this material has been measured under such a high pressure. A new high pressure structure has been observed and all the tentative structure solutions have been tested. We conclude that there is an orthorhombic structure with space group $Cmcm$, based on a weak (110) reflection. Without this information, only available through a

highly sensitive area detector, the structure solution would not be fully determined. The observed structural phase transition of $CuInSe_2$ from the NaCl-like to *Cmcm* at the higher pressure is similar to some of their analogue binary III–V and II–VI groups, for example InP, InAs, ZnSe, CdS, CdSe, HgSe and HgTe [15, 16]. A similar transition sequence has also been reported in other ternary compounds with I–III–VI_2 and II–IV–V_2 chalcopyrite structures [17]. A fact that supports this observation is the tetrahedral bonding of these compounds at ambient pressure, for which the cohesive energy favours the high-symmetry structure of increasing coordination to the rock-salt and *Cmcm* structures in binary III–V and II–VI semiconductors and ternaries such as $CuInSe_2$.

Acknowledgments

We thank Roberts M A of the SRS for assistance in performing the diffraction experiments. We would also like to express our thanks to our colleagues Falconi S and Lundegard L F for their assistance with some of the data collection. This work was supported by the Thai Government Stimulus Package2 (TKK2555), under the Project for Establishment of Comprehensive Centre for Innovative Food Health Products and Agriculture, Research Funds from the Faculty of Science, Chulalongkorn University, the Asahi Glass Foundation and Thailand Research Fund contract number MRG4980031 and DBG5280002. The synchrotron powder diffraction facilities were provided by Daresbury Laboratory. TB acknowledge research grant supported by National Research Council of Thailand.

References

[1] Alonso M I, Wakita K, Pascual J, Garriga M and Yamamoto N 2001 *Phys. Rev.* B **63** 075203
[2] Parlak C and Reyiğit R 2002 *Phys. Rev.* B **66** 165201
[3] Lange P, Neff H, Fearheiley M and Bachmann K J 1985 *Phys. Rev.* B **31** 4074
[4] Rincón C and Bellabarba C 1986 *Phys. Rev.* B **33** 7160
[5] Tinoco T, Pollian A, Gómez D and Itié J P 1996 *Phys. Status Solidi* b **198** 433
[6] González J and Rincón C 1989 *J. Appl. Phys.* **65** 2031
[7] Shock H W 1996 *Appl. Surf. Sci.* **92** 606
[8] Mullan C A, Kiely C J, Casey S M, Imanieh M, Yakushav M V and Thomlinson R D 1997 *J. Cryst. Growth* **171** 415
[9] Chatraphorn S, Yoodee K, Songpongs P, Chityuttakan C, Sayavong K, Wongmanerod S and Holtz P O 1998 *Japan. J. Appl. Phys.* **37** L269
[10] Nelmes R J and McMahon M I 1994 *J. Synchrotron Radiat.* **1** 69
[11] Adams D M 2001 *Diacell Products* 54 Ash Tree Road, Leicester, UK
[12] Mao H K, Bell P M, Shaner J W and Steinberg D J 1978 *J. Appl. Phys.* **49** 3279
[13] Larson A C and Von Dreele R B 2000 General structure analysis system (GSAS) *Los Alamos National Laboratory Report* LAUR 860748
[14] Louër D and Vargas R 1982 *J. Appl. Crystallogr.* **15** 542
[15] Nelmes R J and McMahon M I 1996 *Semicond. Semimetals* **54** 112
[16] McMahon M I and Nelmes R J 1996 *Phys. Status Solidi* b **198** 389
[17] Mori Y and Takarae K 2001 *Ternary and Multinary Compounds in the 21st Century* vol 1 (Tokyo: Institute of Pure and Applied Physics) p 175
[18] Al-Douri Y and Aourag H 2002 *Physica* B **324** 173
[19] Chelikowsky J R and Burdett J K 1986 *Phys. Rev. Lett.* **56** 961

High Pressure Structural Studies of $AgInTe_2$

T Bovornratanaraks[1], K Kotmool[2], K Yoodee[1], M I McMahon[3], D Ruffolo[4]

[1] Department of Physics, Faculty of Science, Chulalongkorn University, Bangkok, 10330, Thailand/ ThEP Center, CHE, 328 Si Ayutthaya Road, Ratchathewi, Bangkok, 10400, Thailand

[2] Department of Physics, Mahidol Wittayanusorn School, 73170, Thailand

[3] SUPA, School of Physics and Astronomy, and Centre for Science at Extreme Conditions, University of Edinburgh, Mayfield Road, Edinburgh, EH9 3JZ, U.K.

[4] Department of Physics, Faculty of Science, Mahidol University, Bangkok, 10400, Thailand/ / ThEP Center, CHE, 328 Si Ayutthaya Road, Ratchathewi, Bangkok, 10400, Thailand

E-mail: thiti.b@chula.ac.th

Abstract. The structural phase transformations in the chalcopyrite semiconductor $AgInTe_2$ have been studied up to 10 GPa on both pressure increase and decrease. The experiments were conducted using angle-dispersive X-ray diffraction with synchrotron radiation and an image plate. The diffraction patterns of $AgInTe_2$ at ambient pressure reveal two coexisting phases: the first has the chalcopyrite structure while the second has a zincblende-like structure. On pressure increase both phases transformed at 3-4 GPa to a cation-disordered orthorhombic structure with spacegroup *Cmcm*. On pressure decrease, the chalcopyrite phase started to reappear at 0.55 GPa, and the *Cmcm* phase disappeared completely at ambient pressure.

1. Introduction

The I-III-VI_2 ternary semiconductors have recently received considerable attention due to their applications in many optoelectronic devices such as solar cells, non-linear opticalal device and detectors [1-2]. The ambient-pressure structure of these compounds is that of chalcopyrite (s.g. I-42d), a doubled zincblende structure which has two distortion parameters that arise due to the difference interactions between the I-VI and III-VI components of the structure. $AgInTe_2$ one member of this I-III-VI_2 group, has been studied under high pressure and temperature and has been reported to have a first-order structural phase transition from chalcopyrite structure to a cation-disorder NaCl-like structure [3-5]. However, our angle-dispersive powder diffraction data reveal a small asymmetric peak shape in all diffraction profiles, and re-investigation on the structure solutions have been carried out in order to fully indentify the high-pressure structure.

2. Experiment

A single crystal of $AgInTe_2$ was prepared by Bridgman method and was ground to a fine powder for the angle-dispersive X-ray diffraction study. High pressure was generated using a diamond anvil cell

© 2010 IOP Publishing Ltd

(DAC) equipped with a tungsten gasket, and with a 4:1 methanol:ethanol mixture as the pressure transmitting medium. The ruby fluorescence method was used to determine the pressure. The diffraction data were collected at the Daresbury Synchrotron Radiation Source (SRS), UK, with wavelength of 0.46540 and 0.44397 Å and an image plate area detector.

3. Results and Discussion

3.1. Ambient Structure

The ambient-pressure diffraction pattern of $AgInTe_2$ is shown in the Figure 1. Using the Rietveld refinement technique with GSAS [6], the sample was found to have the chalcopyrite structure with lattice constants a = 6.39(6) and $_c$ = 12.61(5) Å.. However, several peaks are unindexed by the chalcopyrite structure, as identified by crosses (+) in Fig. 1. These peaks were successfully assigned to a zincblende-like structure, previously reported to be metastable in $AgInTe_2$ at ambient condition [7].

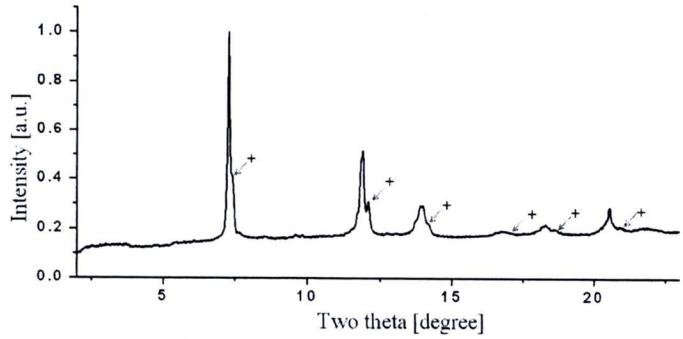

Figure 1 : The X-ray diffraction profiles of AgInTe2 at ambient pressure.

3.2. The High Pressure Structure

The first-order phase transition of $AgInTe_2$ was identified from the X-ray diffraction profiles shown in Figure 2. From ambient pressure up to 2.8 GPa, the diffraction peaks shifted to the higher two theta side but shapes and relative positions remained unchanged. No phase transition thus occurrs over this pressure range. However, at 4.1 GPa, the diffraction peaks of the zincblende phase disappeared and new peaks are emerged. At 6.2 GPa, the chalcopyrite phase also transformed to the same high-pressure phase. The experimental results suggest a transition pressure around 3 to 4 GPa, from the both of the ambient phases to the high-pressure phase.

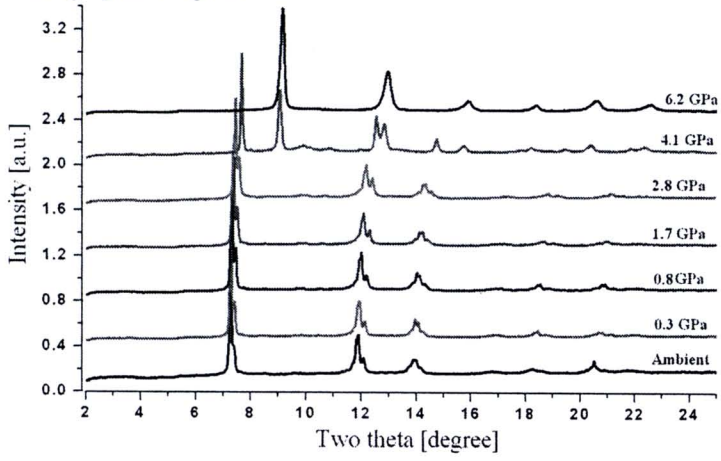

Figure 2 : The X-ray diffraction profiles of $AgInTe_2$ from ambient to 6.2 GPa.

Indexing of the high-pressure phase using DICVOL04 [8], suggested an NaCl-like structure, in agreement with previous reports. However, comparison of the high-pressure phase diffraction pattern with the that calculated from a best-fitting cation-disordered NaCl-like structure and a best-fitting cation-disordered *Cmcm* phase (Figure 3) showed that the data are more consistent with the *Cmcm* structure. At 6.2 GPa, the refined structure of NaCl structure give a lattice parameter of a = 5.87(0) Å with the agreement factors R_{wp} = 4.37 % and R_p = 3.14 %. For the *Cmcm* structure at the same pressure, the atomic coordinates are v = 0.75 for Ag or In and v = 0.25 for Te, with refined lattice parameters a=5.80(8), b=5.79(8), and c=5.87(1) Å. The agreement factors are R_{wp} = 3.45 % and R_p = 2.62 %. The *Cmcm* phase remains stable up to 10.25 GPa. The compressibility is shown in Figure 4, and, using a second order Birch-Murnaghan equation of state, the bulk modulus of the chalcopyrite and *Cmcm* phases are 34.01 and 57.51 GPa, respectively.

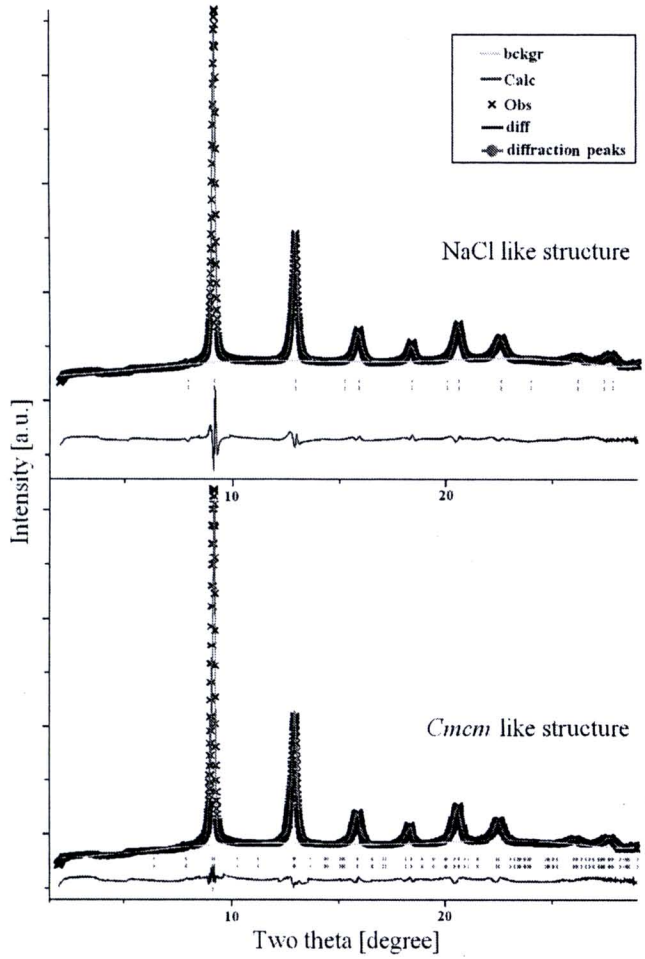

สำนักงานคณะกรรมการวิจัยแห่งชาติ ห้องสมุดงานวิจัย

Figure 3 : Comparison of the refinements between the NaCl-like structure and the *Cmcm* structure at 6.2 GPa. The tick marks show calculated peak positions and the blue like show the differences between calculated and observed profiles.

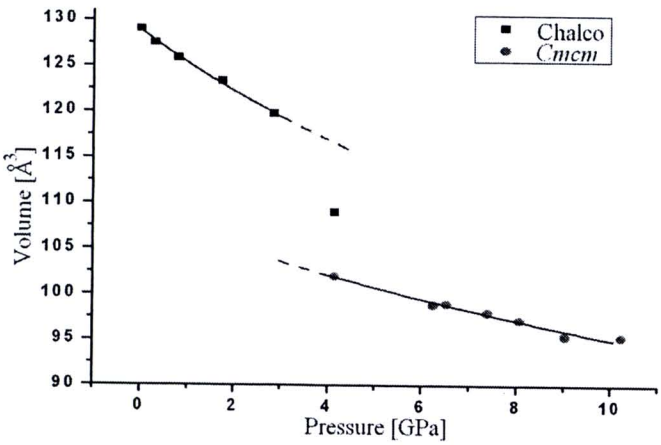

Figure 4 : The pressure-volume diagram of $AgInTe_2$ under high pressure.

On pressure decrease from 10 GPa, the *Cmcm* phase existed down to the ambient pressure but vanished with time. The ambient-pressure profiles only reveal a chalcopyrite structure. The pure chalcopyrite diffraction pattern appeared around 0.55 GPa, where the refined lattice constants of a=6.39(6) and c=12.44(1) Å, were slightly different to those observed on increasing pressure.

4. Conclusion

We have used ADXRD techniques to investigate the crystal structures and phase transitions in $AgInTe_2$ at high pressure. The first structural phase transition occurred around 3 to 4 GPa from two ambient structures, chalcopyrite and a metastable zincblende-like structure, to an *Cmcm* structure. The atomic positions of *Cmcm* structure correspond to an NaCl-like structure, as reported in previuous studies. On pressure decrease, the reverse transition from the *Cmcm* phase to chalcopyrite occurred at a lower pressure than on increasing pressure, and the lattice parameters of the chalcopyrite were slightly different to those observed on pressure increase.

5. Acknowledgement

The authors would like to express their gratitude to the Thailand for National Research Council of Thailand (NRCT). We would also like to express our thank C. Hejny for assistance with the data collection. The synchrotron radiation facilities are provided by the Daresbury Synchrotron Radiation Source (SRS), UK. T.B acknowledges the financial support from Asahi Glass Foundation, National Research Council of Thailand and the Thailand Research Fund contract number 4980031.

References

[1] H. Hann, G Frank, W. Klingler, A. Meyer and G. Storger, *Z. anorg. Chem.* **271**, 153 (1953).
[2] R. Shuka, P. Khurana, and K.K. Srivastara, *J. Mater. Sci.* **3**, 132 (1992).
[3] A. Jayaraman, P.D. Dernier, H.M. Kasper, and R.G. Maines, *High-Temp. High-Pressures.* 9, 97 (1977).
[4] K.J. Range, G. Engert, J. Engels, and A. Weiss *Naturforsch. b* **24**, 1008 (1968).
[5] K.J. Range, and G. Engert, *Sol. State Comm.* **7**, 1749 (1969).
[6] A. C. Larson and R. B. Von Dreele, *Los Alamos National Laboratory Report LAUR*, 2000.
[7] K.J. Range, G. Engert, et al. *Naturforsch. b* **24**, 813 (1969).
[8] Desgreniers S. and K. Lagarec. *J. Appl. Cryst.* **31**, 109 (1998).

Mechanical instabilities and evidence of a medium-range ordered phase in high pressure Strontium using first-principles calculations

P. Srepusharawoot,[1] W. Luo,[2] T. Bovornratanaraks,[3,4] R. Ahuja,[2,5] and U. Pinsook[3,4]

[1] *Department of Physics, Faculty of Science, Khon Kaen University, 40002, Khon Kaen, Thailand*
[2] *Condensed Matter Theory Group, Department of Physics and Astronomy, Uppsala University, Box 516, SE-751 20 Uppsala, Sweden*
[3] *Department of Physics, Faculty of Science, Chulalongkorn University, Bangkok, 10330, Thailand*
[4] *ThEP, Commission on Higher Education, 328 Si-Ayutthaya road, 10400, Bangkok, Thailand*
[5] *Applied Materials Physics, Department of Materials and Engineering, Royal Institute of Technology (KTH), S-100 44 Stockholm, Sweden*

(Dated: January 21, 2011)

We provided the first theoretical evidence for a medium-range ordered phase in high pressure Strontium from the first-principles calculations. At the absolute zero temperature, the enthalpy-pressure relation shows that the bcc and hcp are energetically more favorable than the other experimentally observed phases between 24-27 GPa. In the present work, we concentrate on the bcc phase because we found a link to a medium-range ordered phase. Our results reveal that the bcc phonon dispersion at the N and H points starts softening at around 24.1 GPa. The *ab initio* molecular dynamics at 300 K and 27 GPa showed that the bcc is quickly transformed into a lower energy structure with R3c symmetry. The R3c unit cell looks similar to a hexagonal structure, but with distorted basis. The simulated diffraction patterns showed that the R3c structure has only a single major peak at low angle. The R3c peak locates near the first peak of the bcc structure. This is the evidence of the so-called medium-range ordered phase. This structure is a strong candidate for the unsolved S-phase reported by experiments.

PACS numbers: 64.30.Ef, 71.15.Mb, 81.40.Vw

The X-ray diffraction experiments on Sr under high pressure have been carried out in order to reveal its richness in structural phase transitions. According to the experiments, it has fcc ($Fm\bar{3}m$) structure at ambient pressure, and then transforms into bcc ($Im\bar{3}m$) at 3.5 GPa, β-tin ($I4_1/amd$) at 26 GPa, Sr-IV (Ia) at 35 GPa and Sr-V (I4/mcm) at 46 GPa.[1–5] The fcc→bcc transition is occurred via reversed Bain path.[6] The bcc → β-tin transition was proposed to be a reconstructive phase transition.[7] Furthermore, the β-tin, Sr-IV and Sr-V share some common substructures, and Sr-V is prescribed as an unachieved hcp structure from incomplete Burger mechanism.[7]

However, there is an unsolved structure reported as an S-phase, discovered by Bovornratanaraks *et al.*[5]. It was observed as a coexisted phase during the bcc → β-tin transition in the X-ray diffraction experiments in which the diffraction pattern composed of spotty lines and smooth lines on the Debye-Scherrer rings. The spotty lines are from the crystallographic nature of the material. The smooth lines would come from large number of equivalent planes oriented perfectly random in space. In addition, these smooth lines appeared in the low angles, i.e. $\theta \approx 9.57°$ in $\lambda = 0.4654$ Å. This reflects the medium-range order of the structure, i.e. in the order of few angstroms. The corresponding phase of these smooth lines has been assigned to the S-phase, but the actual structure has been unsolved. A similar smooth lines have been found recently in a glass phase of some alloys under high pressure.[8] Furthermore, the glass phase shares statistical similarities with the melting phase. There was some evidence of room temperature melting under high pressure of some alkaline metals, such as sodium[9].

From first-principles calculations, several studies have been considered for high pressure phases in Sr.[6,10–14] Recent calculations[14] showed that the predicted trend is fcc→bcc→Sr-IV. This discrepancy between calculations and experiments urges us to do more of the in-detail studies. Moreover, the previous studies considered only the enthalpy-pressure (H-P) relationship of various phases except Sr-V phase at absolute zero temperature.

The main aim of this research is as follows; 1. We suggested a possible candidate for the S-phase, found in the experiments.[5] 2. We proposed a mechanism of how S-phase coexists with other high pressure phases. 3. We attempted to give a clue on how to construct the high pressure phases of Sr.

In this work, we calculated the H-P curve of many possible structures of Sr including the incommensurate Sr-V phase, and compared with reported theoretical results[14] of fcc, bcc, beta-tin, and Sr-IV. The H-P curve is calculated by the density functional theory and the projector augmented wave (PAW) method[15,16], as implemented in Vienna Ab initio Simulation Package (VASP)[17,18]. Under the PAW approach, we treated $4s$, $4p$ and $5s$ as valence states. The exchange-correlation potential was derived from Perdew-Wang (PW91) generalized-gradient approximation (GGA) functional.[19] A plane wave cutoff energy of 500 eV is employed. The irreducible Brillouin zone was sampled using Monkhorst-Pack scheme[20], with $9 \times 9 \times 1$ **k**-points for Sr-V and $9 \times 9 \times 9$ **k**-points for the other structures.

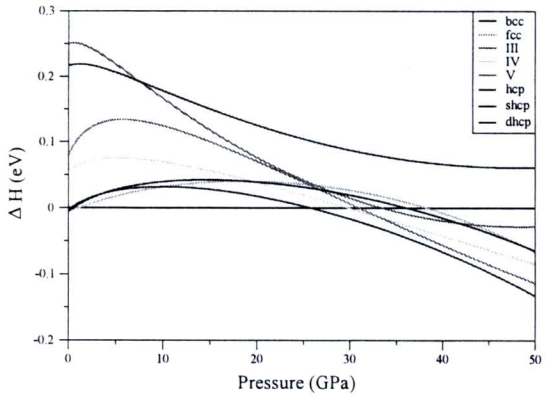

FIG. 1: Enthalpy-pressure relation of several possible phases from *ab initio* calculations. The bcc enthalpy was used as a reference.

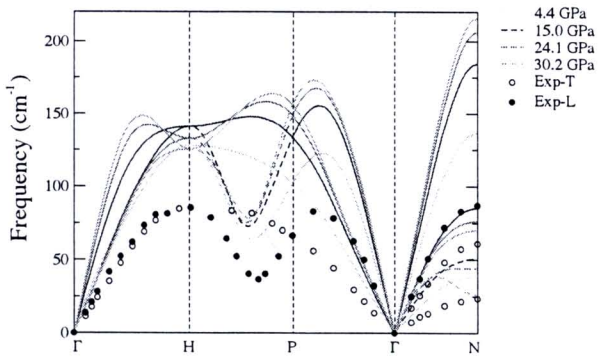

FIG. 2: bcc phonon dispersion at various pressures. At the N and H points, the phonons start softening at 24.1 GPa. The results are compared with the available experimental data at 930K.[24]

The Sr-V supercell has 110 atoms with 14 guest and 10 host unit cells with I4/mcm symmetry. A similar *ab initio* method has been used to calculate the incommensurate phases in Ba-IV[21] and Sc-II[22,23], and gave a good description on their structural phase transitions. The incommensurate ratio (γ) in the c-axis is 1.4 compared with 1.4041 from experiments.[4] The Wyckoff parameter of γ=1.4041 is 8h(x, x+0.5, 0), x=0.14602, taken from the experiment at 56 GPa.[4] At this pressure, the experimental lattice parameters for host structure are a_h=6.9582 Å and c_h=3.9592 Å, and the lattice parameter for guess structure are a_g=6.9613 Å and c_g=2.8201 Å.

Geometry optimization was carried out within the Conjugate-Gradient algorithm and the force acting on each ion was calculated via the Hellmann-Feynman theorem. The equation of states (EOS) was obtained by fitting the total energy of the optimized structure of several different volumes to the third order Birch-Murnaghan EOS. The H-P relation of all studied phases is shown in Figure 1.

From Figure 1, we plotted the H-P relation of fcc, bcc, Sr-III (β-tin), Sr-IV, Sr-V compared with hcp, shcp and dhcp phases. Moreover, we also looked at the bct and bco structures. Our results reveal that the predicted trend is fcc→bcc→hcp. There are several remarkable points; the bcc has the lowest enthalpy upto 25GPa. The next lowest-enthalpy structure is the hcp. Thus the H-P relation suggests that the bcc→hcp transition pressure is around 25GPa. The hcp has energy closed to the fcc at low pressure. This low-pressure behavior of the hcp was seen also in a full potential linear augmented plane wave (FPLAPW) study[13]. The key point here is that the zero kelvin temperature calculations cannot reproduce the experimental phase diagram. This gave us a clue that only absolute zero temperature calculations give inadequate description to the high pressure phase of Sr.

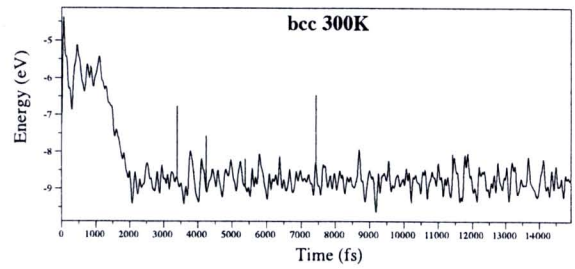

FIG. 3: The AIMD time evolution of the bcc structure. The bcc is stable for 1 ps before undergoing a phase transition to a lower energy phase.

Next, the dynamic contribution are considered. It has been showed that alkali and alkaline-earth metals exhibit severe mechanical instabilities[25–28], i.e. phonon instabilities and elastic softening, which lead to structural phase transitions. Therefore, in order to give more insight into the discrepancy between the calculated phase sequence and the experiments, the mechanical analysis in terms of phonons and molecular dynamics has done extensively in the bcc structure in the pressure range where the discrepancy emerges. Moreover, we believed that the bcc phase might be able to link to the S-phase when time is evolved.

The phonon dispersion curve was calculated using linear response theory via Quantum Espresso code[29]. The linear response theory gives us the phase stability in the harmonic regime. The calculated phonon dispersion relation compared with the available experimental data at 930K[24] of bcc phase is shown in Figure 2. There was a low temperature measurement of the bcc phonons[30] as well but data points were unavailable. The phonon hardening under pressure can be obviously observed and it can

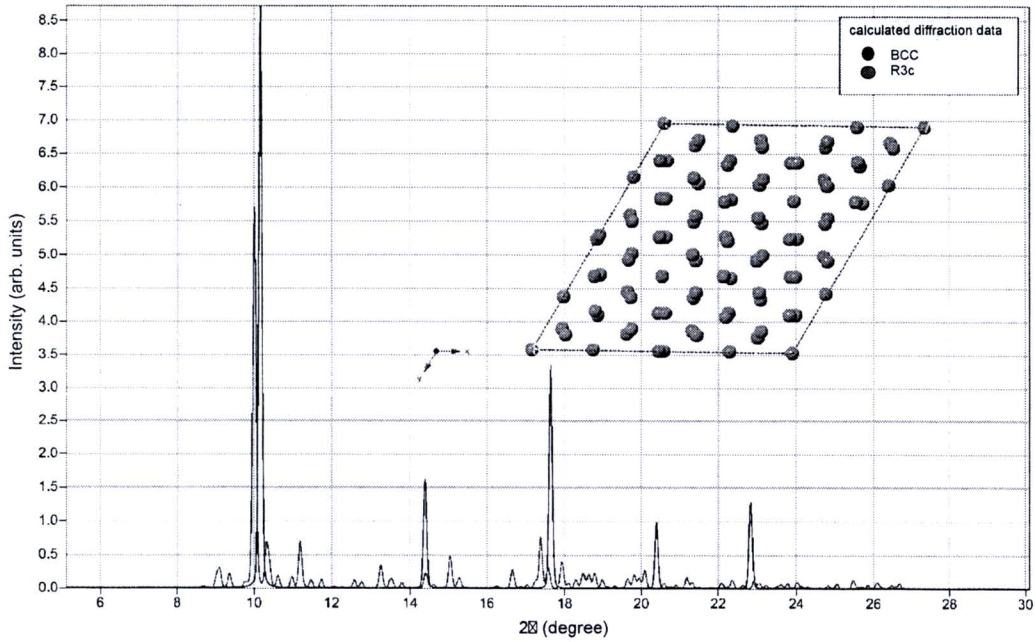

FIG. 4: (A) The typical configuration of the R3c structure. (B) the simulated X-ray diffraction of the R3c structure (black) compared with the bcc structure at 27 GPa (red).

be seen also in the studies of alkaline metals.[27,28] According to Figure 2, we found that the calculated bcc phonons are stable at low pressure. At around 24.1 GPa, phonons at the N and H-points start softening. It was shown before that the softening of the N-point phonons leads to a bcc-hcp phase transition in zirconium[31]. However, the H-point phonons are also softening a little. According to the H-P relation and the phonon calculations, there is a strong tendency that the bcc Sr would transform into the hcp or other lower symmetry structures. Then, we used AIMD simulations to carify this point.

At the final stage, we consider full dynamics of the system, using AIMD simulations.[17,18] This is because Strontium, in particular, was shown to exhibit anomalously anharmonic effects.[25] Underestimating anharmonicity in the dynamical contribution results in incorrect P-T phase boundary in the fcc→bcc phase transition in Sr.[32] It is indicated that the full dynamics can be responsible for the discrepancy between the previous theoretical prediction and experimental phase diagram.

The AIMD was performed using NVT ensembles, periodic boundary condition and Gamma-point sampling. The same method was used in the study of Na melting under high pressure.[9] The bcc supercell contained 64 atoms of Sr. The fully relaxed structures at 27 GPa were used as an initial configuration. This pressure is just beyond the stability region of the bcc phonons. The integration timestep was 1 fs and it was integrated upto 15 ps. Temperature was set at 300 K and regulated by the velocity rescaling every time step. The time evolution of the bcc supercell were shown in Figure 3.

According to Figure 3, we found that the bcc structure is stable for 1 ps only. Then it undergoes a phase transition to a lower energy structure, i.e. the energy difference compared with the bcc is about -0.05 eV/atom. From the symmetry determination of the final structure obtained from the AIMD, we found that the transforming phase belongs to R3c space group. The structural parameters of this structure are $a = b = 21.3470$ Å and $c = 6.2436$ Å, $\alpha = \beta = 90°$, and $\gamma = 120°$, as shown in Figure 4 (a). The positions of Sr atoms are as follows: Sr1=(-0.164,-0.570,0.316), Sr2=(0.169,-0.402,-0.698), Sr3=(0.003,-0.490,-0.309), Sr4=(-0.402,-0.328,-0.042), Sr5=(0.236,-0.002,-0.206), and Sr6=(0,0,-0.681). From our symmetry analysis, it can be seen that this structure is a hexagonal lattice with distorted basis. Then, we calculate the diffraction pattern with $\lambda = 0.4654$ Å. The results were shown in Figure 4 (B), compared with the bcc structure (red curve). The first peak of the bcc is at 10.17°. The R3c structure has only one major peak at 10.01°, which corresponding to orderness of a range of a few angstrom. As mentioned earlier, the experimental diffraction pattern consisted of very smooth lines at 9.57° in Debye-Scherrer rings. This should be corresponding to a phase with some limited degree of orderness. This feature can be fitted with the R3c structure from AIMD, except the position of the diffraction peak which is 0.44° higher than the experimental values.

From our findings, we can suggest phase coexistence scenario where 1) the bcc is mechanically unstable and transformed into the distorted hexagonal structure, with R3c symmetry. 2) We found from the H-P relation that the hcp is energetically favorable. It could be a suggestion for further studied of other hcp-like structures. Furthermore, the Sr-III, Sr-IV and Sr-V structures were believed to be a result of incomplete Burger mechanism.[7] There must be a link between the hcp and high pressure phases of Sr. 3) We also showed that the full dynamics of Sr is significant in correctly describing high pressure phase transitions. In order to correctly reproducing the high pressure phase diagram, the full dynamics must be fully taken into the account.

Acknowledgments

The authors would like to express their gratitude to H.K. Mao for his valuable discussion on the glass phase during the EHPRG-48 conference. P.S. and U.P. would like to thank A.Phusittrakool for bringing this problem into their attention. R.A. and U.P. were supported by VR-SIDA during the research in Sweden. T.B. and U.P. would like to express their gratitude to the national research council of Thailand (NRCT) and A1B1 funding from Faculty of Science, Chulalongkorn university. T.B. acknowledges the financial support from Asahi Glass Foundation and Thailand Research Fund contract number DBG5280002, and would like to acknowledge ICTP also for funding through associateship scheme.

[1] H. Olijnyk and W. B. Holzapfel, Phys. Lett. A **100**, 191 (1984).
[2] M. Winzenick and W. B. Holzapfel, Phys. Rev. B **53**, 2151 (1996).
[3] D. R. Allan, R. J. Nelmes, M. I. McMahon, S. A. Belmonte, and T. Bovornratanaraks, Rev. High Pressure Sci. Technol. **7**, 236 (1998).
[4] M. I. McMahon, T. Bovornratanaraks, D. R. Allan, S. A. Belmonte, and R. J. Nelmes, Phys. Rev. B **61**, 3135 (2000).
[5] T. Bovornratanaraks, D. R. Allan, S. A. Belmonte, M. I. Mcmahon, and R. J. Nelmes, Phys. Rev. B **73**, 144112 (2006).
[6] V. L. Sliwk, P. Mohn, K. Schwarz, and P. Blaha, J. Phys.: Condens. Matter **8**, 799 (1996).
[7] H. Katzke and P. Tolédano, Phys. Rev. B **75**, 174103 (2007).
[8] Q. S. Zeng, Y. Ding, W. L. Mao, W. Luo, A. Blomqvist, R. Ahuja, W. Yang, J. Shu, S. V. Sinogeikin, Y. Meng, et al., Proc. Natl. Acad. Sci. U.S.A **106**, 2515 (2009).
[9] L. Koci, R. Ahuja, L. Vitos, and U. Pinsook, Phys. Rev. B **77**, 132101 (2008).
[10] H. L. Skriver, Phys. Rev. Lett. **49**, 1768 (1982).
[11] R. H. Mutlu, Phys. Rev. B **54**, 16321 (1996).
[12] R. Ahuja, B. Johansson, and O. Eriksson, Phys. Rev. B **58**, 8152 (1998).
[13] F. Jona and P. M. Marcus, J. Phys.: Condens. Matter **18**, 4623 (2006).
[14] A. Phusittrakool, T. Bovornratanaraks, R. Ahuja, and U. Pinsook, Phys. Rev. B **77**, 174118 (2008).
[15] P. Blöchl, Phys. Rev. B **50**, 17953 (1994).
[16] G. Kresse and J. Joubert, Phys. Rev. B **59**, 1758 (1999).
[17] G. Kresse and J. Hafner, Phys. Rev. B **47**, 558 (1993).
[18] G. Kresse and J. Furthmüller, Phys. Rev. B **54**, 11169 (1996).
[19] J. P. Perdew and Y. Wang, Phys. Rev. B **45**, 13244 (1992).
[20] H. J. Monkhorst and J. D. Pack, Phys. Rev. B **13**, 5188 (1976).
[21] S. K. Reed and G. J. Ackland, Phys. Rev. Lett. **84**, 5580 (2000).
[22] A. Ormeci, K. Koepernik, and H. Rosner, Phys. Rev. B **74**, 104119 (2006).
[23] S. Arapan, N. V. Skorodumova, and R. Ahuja, Phys. Rev. Lett **102**, 085701 (2009).
[24] J. Mizuki and C. Stassis, Phys. Rev. B **32**, 8372 (1985).
[25] V. G. Vaks, G. D. Samolyuk, and A. Y. Trefilov, Phys. Lett. A **127**, 37 (1988).
[26] V. G. Vaks, M. I. Katsnelson, A. I. Likhtenstein, G. V. Peschanskikh, and A. V. Trefilov, J. Phys.:condens. Matter **3**, 1409 (1991).
[27] Y. Xie, J. S. Tse, T. Cui, A. R. Oganov, Z. He, Y. M. Ma, and G. Zou, Phys. Rev. B **75**, 064102 (2007).
[28] Y. Xie, Y. M. Ma, T. Cui, Y. Li, J. Qiu, and G. T. Zou, New J. Phys. **10**, 063022 (2008).
[29] P. Giannozzi *et al.* `http://www.quantum-espresso.org`.
[30] U. Buchenau, M. Heiroth, H. R. Schober, J. Evers, and G. Oehlinger, Phys. Rev. B **30**, 3502 (1984).
[31] U. Pinsook and G. J. Ackland, Phys. Rev. B **59**, 13642 (1999).
[32] J. A. Moriarty, Phys. Rev. B **8**, 1338 (1973).